

Localization of electrons in multiple layers of self-assembled GeSi/Si islands

A. I. Yakimov,* A. I. Nikiforov, and A. V. Dvurechenskii

*Institute of Semiconductor Physics,
Siberian Branch of the Russian Academy of Sciences,
prospekt Lavrent'eva 13, 630090 Novosibirsk, Russia*

(Dated: July 25, 2006)

Abstract

Space-charge spectroscopy was employed to study electronic structure of single and multiple layers of GeSi islands embedded in an n -type Si(001) matrix. For a multilayer sample, the evidence for an electron localization in strained Si in the vicinity of GeSi dots was found. From the temperature- and frequency-dependent measurements the electron binding energy was determined to be 40–70 meV. The electron accumulation was not observed in a sample with a single layer of GeSi islands. Existence of localized electronic states is explained by a modification of the conduction band alignment induced by inhomogeneous tensile strain in Si around the buried GeSi dots.

PACS numbers: 73.21.La, 73.20.At, 71.70.Fk, 81.07.Ta

*Electronic address: yakimov@isp.nsc.ru

There are two main types of band-edge alignment, namely type-I and type-II, in heterostructures with semiconductor quantum dots (QD's). In type-I QD's, the band gap of the narrow-gap material lies entirely within the gap of the wide-gap semiconductor, and both electron and hole are confined inside the same region. A typical example of type-I band-edge line-up is the InAs QD's in GaAs matrix. For type-II QD's, the localization inside the dot occurs only for one of the charge carriers, whereas the dot forms a potential barrier for the other particle. A system like this is that of Ge/Si(001) dots formed by strain epitaxy, in which the holes are strongly confined in the Ge region, and the electrons are free in the Si conduction band. The above consideration disregards possible modification of the band structure due to inhomogeneous strain in the dots and the surrounding matrix. Tensile strain in the nearby Si causes splitting of the sixfold-degenerate Δ_6 -valleys (Δ_6) into the fourfold-degenerate in-plane Δ_4 -valleys and the twofold-degenerate Δ_2 -valleys along the [001] growth direction. [1–4] The lowest conduction band edge just above and below the Ge island is formed by the Δ_2 -valleys yielding the triangle potential well for electrons in Si near the Si/Ge boundary. Thus one can expect three-dimensional localization of electrons in the strained Si near the Ge dots. The electron binding energy in a strain-induced potential well in a single Ge/Si QD was predicted to be very small (< 10 meV). [2] This value is expected to enlarge vastly in multilayer Ge/Si structures with vertical stacking of Ge islands due to accumulation of strain energy from different dot layers in a stack and increase of the potential well depth. In this work we employ space-charge spectroscopy to look for the evidence of the electron accumulation in samples with a single layer of GeSi islands and with a stack of four layers of GeSi QD's embedded in an n -type Si(001) matrix.

GeSi/Si heterostructures with self-assembled GeSi islands were fabricated by molecular-beam epitaxy in the Stranskii-Krastanov growth mode on a n^+ -Si(001) substrate with a resistivity of $0.01 \Omega \text{ cm}$ doped with antimony up to a concentration of $\sim 10^{19} \text{ cm}^{-3}$. A fourfold stack of GeSi islands was inserted into the $0.8\text{-}\mu\text{m}$ epitaxial n -Si layer at a distance of $0.5 \mu\text{m}$ from the substrate. The amount of deposited Ge in each QD layer was about 6 monolayers (MLs, $1 \text{ ML}=1.457 \text{ \AA}$), the Ge growth rate was chosen to be as large as 2 ML/s to ensure the high Ge content in the islands and hence the large strain. The n -type remote doping was achieved by insertion of a Sb δ -doping Si layer $0.2 \mu\text{m}$ below the GeSi QD layer. The first and second Ge layers in the stack as well as the third and fourth Ge layers are separated by 3 nm Si spacers, while the distance between the second

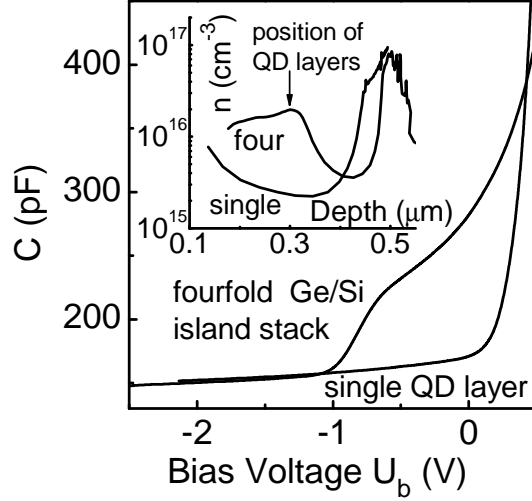


FIG. 1: Capacitance-voltage characteristics measured at modulation frequency of 10 kHz and at $T = 77$ K for the single-layer and multilayer samples. The inset displays the apparent electron distribution derived from the measured C - V curves using the full depletion approximation.

and third Ge layers is 5 nm. Ge nanoclusters fabricated by such a way demonstrate good vertical correlation. From cross-sectional transmission electron micrographs, we observe the GeSi dots to be approximately 20 nm in lateral size and about 2 nm in height. The scanning tunneling microscopy of a sample without the Si cap layer showed that the Ge islands have a shape of hut-clusters. The density of the dots is about 10^{11} cm^{-2} . The average Ge content of 80% in the islands was determined from Raman measurements. To separate response from the stacked Ge/Si islands, the reference sample was fabricated under conditions similar to the multilayer sample, except that only a single layer of GeSi QDs was grown. For the capacitance and conductance measurements, Pd Schottky gates with the area of 7.5×10^{-3} cm^2 were deposited on top of the samples through a shadow mask. The admittance was measured using a Fluke PM6306 Meter in the frequency range $f = 10$ –1000 kHz at temperatures from 4 to 150 K. The amplitude of the ac modulation voltage was 50 mV.

Figure 1 shows experimental capacitance-voltage (C - V) characteristics for the reference and the multilayer samples. The dependence of the capacitance on voltage for the single-layer sample shows no specific features and has the form of the conventional C - V characteristic of an n -type Schottky diode. For the multilayer sample, we observe a steplike structure caused by an additional capacitance, which we associate with the negative charge accumulation in

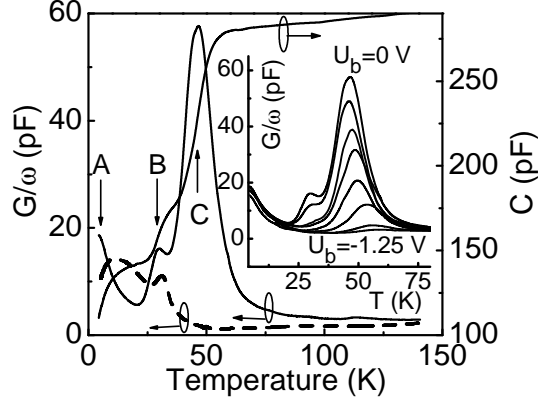


FIG. 2: Temperature dependence of conductance (G) and capacitance (C) measured at bias voltage $U_b = 0$ V and modulation frequency of 1 MHz for the single-layer sample (broken line, only conductance is shown) and fourfold Ge/Si island stack (solid lines). Inset: Conductance spectra of the multilayer sample at the frequency of 1 MHz under different bias voltages. The voltages are 0 V, -0.2 V, -0.5 V, -0.7 V, -0.9 V, -1.0 V, -1.2 V, and -1.25 V from top to bottom.

the Si layers between the stacked Ge islands (see, inset of Fig. 1). Due to the n -type doping in the Si matrix, the stacks of GeSi QD's will be charged by electrons at a zero bias. When a reverse bias is applied to the diode, the electrons are gradually swept out. At $U_b > 1$ V electrons escape from the stack of GeSi/Si dots and the latter become neutral.

The QD contribution to the capacitance disappears at temperatures below ~ 50 K (Fig. 2) due to "freezing" the electrons in the $\Delta 2$ bound states in the strained Si. The corresponding step on the temperature dependence of capacitance is accompanied by the conductance maximum (peak C in Fig. 2) which is not seen for the reference sample. Thus we may attribute the conductance peak C to the ac response of electrons confined in GeSi/Si islands stacked in a multilayer structure. With increasing reverse bias, the position of peak C shifts towards higher temperatures, its amplitude gradually decreases and the peak disappears at voltages $|U_b| > 1$ V just after the ending of the QD-related capacitance plateau in C - V characteristic. Peaks A and B are observed in both samples. They are assigned to a dopant-related admittance signal associated with the carrier freeze-out effect in the highly doped δ -doping Si layer (peak A) and in Si layers with a lower doping Sb concentration (peak B). [4, 5]

Typical conductance spectra measured at different frequencies are shown in Fig. 3. Admittance signal originated from electron traps can be used to extract the electron energy

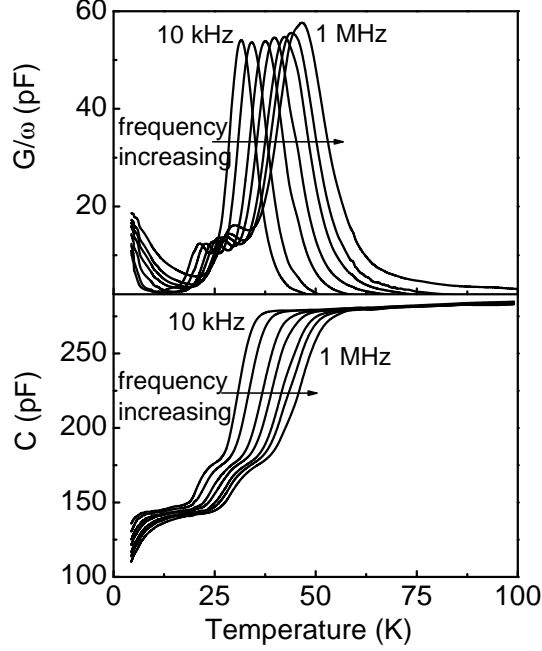


FIG. 3: Conductance and capacitance spectra of the multilayer QD sample at the bias voltage of 0 V under different modulation frequencies. The frequencies are 10 kHz, 30 kHz, 100 kHz, 200 kHz, 400 kHz, 600 kHz, and 1 MHz.

level. [6] For a given measurement frequency $\omega = 2\pi f$, the conductance reaches a maximum at a temperature T_{\max} which corresponds to the condition $e_n(T_{\max}) \approx \omega/2$, where $e_n = e_0 \exp(-E_a/kT)$ is the emission rate of electrons from the bound to extended states which depends on the electron binding energy E_a . Thus, by measuring $G(T)$ dependencies at various ω , the activation energies of the electron emission rate can be deduced from the Arrhenius plots of $e_n(T_{\max})$ vs $1/T_{\max}$. Arrhenius plots necessary for deriving the activation energy are depicted in inset of Fig. 4. The activation energies of the electron emission rate were found from the slope of the approximating straight lines. The resulting values of E_a are shown in Fig. 4 as a function of reverse bias voltage.

To support experimental results we performed numerical analysis of three-dimensional strain distribution and electronic structure of the samples under investigation. The strain distribution was found in terms of atomic positions using valence-force-field model with a Keating interatomic potential. [7] The electronic energy levels were calculated by solving three-dimensional effective-mass Schrödinger equation by means of a free-relaxation method. [8] The carrier confinement potential in this equation is modified by the strain

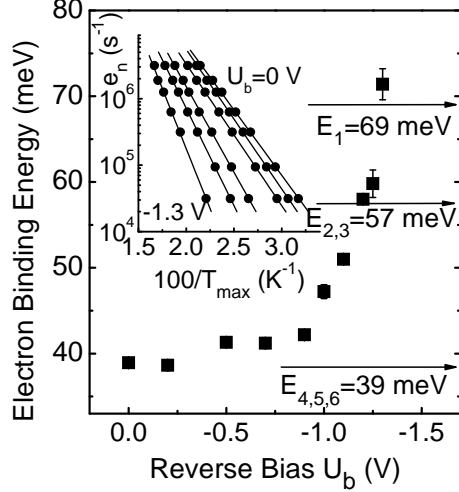


FIG. 4: Bias dependent activation energies of electron emission rate. The arrows show the calculated electron binding energies. Inset displays the Arrhenius plots of the electron emission rate e_n obtained from G - T spectra with different bias voltages. The voltages are 0 V, -0.5 V, -0.9 V, -1.1 V, -1.2 V, and -1.3 V.

distribution. Details of theoretical consideration can be found elsewhere. [4] In Fig. 5 we show the isosurface plots of the charge density for the first 6 electronic states with the respective electron binding energies E_i . The same energies are shown in Fig. 4 by arrows. Obviously, the calculated values of E_i agree well with the experimental data providing the evidence for the electron confinement in GeSi/Si QD's stacked in a multilayer structure.

The authors are much obliged to V. A. Volodin for Raman measurements, A. A. Bloshkin and A. V. Nenashev for numerical simulation of electronic structure. This work was supported by the Russian Foundation for Basic Research (Grant No. 06-02-16143), State Contract No. 02.442.11.7282, and the Integration Project of Siberian Branch of the Russian Academy of Sciences (No. 101).

-
- [1] O. G. Schmidt, K. Eberl, Y. Rau, Phys. Rev. B **62**, 16715 (2000).
[2] A. I. Yakimov, N. P. Stepina, A. V. Dvurechenskii, A. I. Nikiforov, A. V. Nenashev, Semicond. Sci. Technol. **15**, 1125 (2000).
[3] J. H. Seok, J. Y. Kim, Appl. Phys. Lett. **78**, 3124 (2001); J. Y. Kim, J. H. Seok, Mater. Sci. Eng. B **89**, 176 (2002).

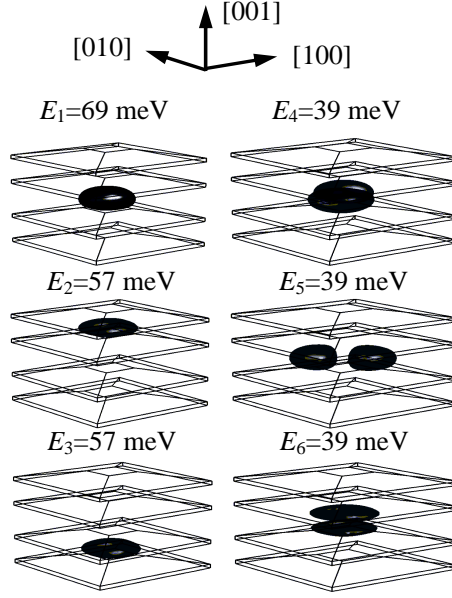


FIG. 5: Three-dimensional view of the isosurface of the electron charge density for the six lowest conduction states. The isosurface level is selected as $1/e$ ($e = 2,71828\dots$) of the maximum wavefunction amplitude $|\psi_{max}(\mathbf{r})|$. The probability of finding the electron inside is 70–77% dependent on the state. E_i is the single-electron binding energy of the i -th state, determined with the error of ± 1 meV.

- [4] A. I. Yakimov, A. V. Dvurechenskii, A. I. Nikiforov, A. A. Bloshkin, A. V. Nenashev, and V. A. Volodin, *Phys. Rev. B* **73**, 115333 (2006).
- [5] D. V. Singh, R. Kim, T. O. Mitchell, J. L. Hoyt, and J. F. Gibbons, *J. Appl. Phys.* **85**, 985 (1999).
- [6] W.-H. Chang, W. Y. Chen, M. C. Cheng, C. Y. Lai, T. M. Hsu, N.-T. Yeh, and J.-I. Chyi, *Phys. Rev. B* **64**, 125315 (2001).
- [7] P. N. Keating, *Phys. Rev.* **145**, 637 (1966).
- [8] F. B. Pedersen, Yia-Chung Chang, *Phys. Rev. B* **53**, 1507 (1996).